

IN-1185
October 1968

73835

CORROSION EXPERIENCE WITH TYPE 316 STAINLESS STEEL
IN SODIUM-POTASSIUM EUTECTIC ALLOY AT 1400°F

AMPTIAC

DISTRIBUTION STATEMENT A
Approved for Public Release
Distribution Unlimited



IDAHO NUCLEAR CORPORATION
NATIONAL REACTOR TESTING STATION
IDAHO FALLS, IDAHO

Reproduced From
Best Available Copy

DTIC QUALITY INSPECTED 4

20000906 099

U. S. ATOMIC ENERGY COMMISSION

Printed in the United States of America
Available from
Clearinghouse for Federal Scientific and Technical Information
National Bureau of Standards, U. S. Department of Commerce
Springfield, Virginia 22151
Price: Printed Copy \$3.00; Microfiche \$0.65

LEGAL NOTICE

This report was prepared as an account of Government sponsored work. Neither the United States, nor the Commission, nor any person acting on behalf of the Commission:

A. Makes any warranty or representation, express or implied, with respect to the accuracy, completeness, or usefulness of the information contained in this report, or that the use of any information, apparatus, method, or process disclosed in this report may not infringe privately owned rights; or

B. Assumes any liabilities with respect to the use of, or for damages resulting from the use of any information, apparatus, method, or process disclosed in this report.

As used in the above, "person acting on behalf of the Commission" includes any employee or contractor of the Commission, or employee of such contractor, to the extent that such employee or contractor of the Commission, or employee of such contractor prepares, disseminates, or provides access to, any information pursuant to his employment or contract with the Commission, or his employment with such contractor.

IN-1185
Issued: October 1968
Metals, Ceramics and Materials
TID-4500

CORROSION EXPERIENCE WITH TYPE 316 STAINLESS STEEL
IN SODIUM-POTASSIUM EUTECTIC ALLOY AT 1400°F

by

T. L. Hoffman

IDAHO NUCLEAR CORPORATION

A JOINTLY OWNED SUBSIDIARY OF
AEROJET GENERAL CORPORATION ALLIED CHEMICAL CORPORATION



U. S. Atomic Energy Commission Research and Development Report
Issued Under Contract AT(10-1)-1230
Idaho Operations Office

ACKNOWLEDGEMENTS

The following persons from the Nuclear and Chemical Technology Division of Idaho Nuclear Corporation made significant contributions to the test material appearing in this report:

E. S. Dickerson

K. C. Sumpter

G. E. Lohse

W. F. Zelezny

The investigation of thermal stresses at the expansion tank connections in the sodium-potassium piping system located in the Waste Calcining Facility was conducted by T. K. Burr, Engineering Division of Idaho Nuclear Corporation.

ABSTRACT

Service test examinations were performed on the Type 316 stainless steel loop for circulating sodium-potassium (NaK) eutectic alloy in the Waste Calcining Facility at the Idaho Chemical Processing Plant. These examinations of the stainless steel loop revealed the cumulative effects of 24,300 hours of operation at temperatures of 1100-1400°F during the last six years. Although Type 316 stainless steel performed satisfactorily and is still being used in this service, the results showed that changes in mechanical properties and metallurgical effects occur with circulating non-isothermal NaK in contact with Type 316 stainless steel. Some mass transfer of alloying elements from the hot regions of the Type 316 stainless steel loop to the colder regions was observed. The mitigation of these effects is discussed.

CONTENTS

	page
ACKNOWLEDGEMENTS.	ii
ABSTRACT.	iii
SUMMARY	vii
I. INTRODUCTION.	1
II. GENERAL CONSIDERATIONS ON THE MECHANISMS OF CORROSION IN LIQUID NaK	3
1. SENSITIZATION	3
2. SIGMA PHASE FORMATION	3
3. MASS TRANSFER	5
III. NaK LOOP IN THE WASTE CALCINING FACILITY.	7
IV. EXPERIMENTAL PROCEDURES	9
V. RESULTS	12
1. PIPE SECTION.	12
2. FITTINGS.	18
2.1 Connector Failure After 3,600 Hours Total Service. .	18
2.2 Connector Failure After 17,024 Hours Total Service .	19
2.3 Thermal Stress Analysis.	26
2.4 Failure of Reducer in NaK Drain Piping	26
3. ELECTROMAGNETIC PUMP.	29
VI. CONCLUSIONS	34
VII. REFERENCES.	35
APPENDIX -- ANALYSIS AND TENSILE STRENGTH OF STEEL USED IN THE WCF.	37

FIGURES

	page
1. Fluidized bed waste calcining facility.	2
2. NaK system flow diagram	8
3. Sheet tensile specimen.	10
4. Impact test specimen.	10
5. Tube tensile specimen	11
6. Sigma particle in cross-section of Type 316 ss pipe after 15,000 hours service at about 1400°F	15
7. Cross-section of Type 316 ss pipe after 15,000 hours service at about 1400°F.	15
8. Decarburized zone of inside edge of 3-inch Sch 40 Type 316 ss pipe after 15,000 hours service at about 1400°F	16
9. Air-side of Type 316 ss pipe after 15,000 hours service at about 1400°F.	16
10. NaK expansion tank weld failure after 3,240 hours at 1100-1400°F service	16
11. Connector weld failure after 3,240 hours at 1100-1400°F	18
12. Surface topography of nozzle-connector weld failure after 3,240 hours at 1100-1400°F showing crack front arrest lines	19
13. Cross-section through tee connector weld.	20
14. Cross-section through wrought connector	21
15. Internal crack in wall of pipe tee connector showing transgranular propagation after 15,800 hours service at about 1100-1400°F . .	21
16. Crack on inside of pipe tee connector after 15,800 hours of service at about 1100-1400°F.	21
17. Internal crack in wall of connector. (Same area shown in Figure 16).	22
18. Internal crack in wall of connector. (Same area shown in Figure 16).	22
19. Inside of pipe tee after 45 sec. Vilella etch	23
20. Inside of pipe tee after 30 sec. Vilella etch	23
21. Surface topography of outside crack at the pipe tee connector weld.	25
22. Surface topography produced by tearing material beyond the crack	25
23. Surface topography of inside crack at the pipe tee connector weld.	25

24.	Diagram of 3-inch x 1½-inch eccentric reducer	26
25.	Decarburized zone of the inside surface of the reducer after 19,100 hours at about 1100-1400°F	27
26.	Grain dropping in the decarburized zone of the reducer after 19,100 hours at about 1100-1400°F	27
27.	Root of the turkey foot crack on the inside surface of the reducer after 19,100 hours at about 1100-1400°F	28
28.	Weld showing sigma phase formation after 19,100 hours at about 1100-1400°F	28
29.	Cross-section of forging showing intergranular fracturing after 19,100 hours at about 1100-1400°F	28
30.	Surface topography of the weld failure at the reducer to 1-inch pipe after 19,100 hours at about 1100-1400°F.	28
31.	Surface topography of the crack of the forged reducer after 19,100 hours service at about 1100-1400°F	29
32.	NaK electromagnetic pump.	30
33.	Dismantled NaK electromagnetic pump tube and armature coil. . .	31
34A.	Inside surface of NaK EM pump tube after 20,100 hours at 1022- 1400°F.	32
34B.	Inside surface of pin hole failure of the EM pump tube.	32
34C.	Inside surface opposite the pin hole of the EM pump tube. . . .	32
35.	Cross-section of pin hole in NaK pump tube after 20,100 hours at about 1022-1100°F.	33
36.	Cross-section of pit in NaK pump tube after 20,100 hours at about 1022-1400°F	33
37.	Cross-section of EM pump tube showing a carburization band on the NaK side of pump tube after 20,100 hours at about 1022-1100°F .	33
38.	Cross-section of EM pump tube showing carburization on NaK side of pump tube after 20,100 hours at about 1022-1100°F.	33

TABLES

I.	Corrosion of Wrought Type 316 Stainless Steel Pipe in Boiling 65 Percent Nitric Acid After 16,292 Hours Service in NaK at 1400°F.	14
II.	Mechanical Properties of Type 316 Stainless Steel	17

Start

SUMMARY

The Waste Calcining Facility (WCF) at the Idaho Chemical Processing Plant employs a fluidized bed calcination process for converting highly radioactive aqueous waste into granular solids. Heat is supplied to the calciner by circulating sodium-potassium (NaK) eutectic alloy at 1400°F through a bayonet heat exchanger in the fluidized bed of solids. Construction material for the NaK loop in the WCF is Type 316 stainless steel; the bayonet heat exchanger is Type 316 stainless steel modified with columbium and tantalum. As of November 13, 1967, this loop had been in service for 1,327 hours below 1100°F and 24,309 hours between 1100°F and 1400°F, with 46 startups from room temperature.

As part of the overall program of surveillance on the NaK loop, service tests were made on several fittings, on an electromagnetic pump, and on a portion of the piping. The results showed that small mass transfer effects, resulting in the removal of carbon from the hot regions of the loop and the deposition of carbon in the colder regions, are encountered with NaK circulated under non-isothermal conditions in contact with Type 316 stainless steel. Analysis showed that about one mil of decarburization had occurred on the NaK side of the piping that was in the hot region and about five mils of carburization was present on the NaK electromagnetic pump tube which was in the colder region of the loop. Sigma growth was present in the cross-section of the pipe just beyond the decarburized layer. Diamond-pyramid hardness values of exposed pipe were not significantly different from values for unexposed pipe. Tensile tests on the exposed material revealed no significant loss in tensile strength; however, elongation decreased approximately 43% at room temperature and approximately 63% at 1400°F. The exposed pipe cracked badly during an ASTM A 376 flattening test, while unexposed pipe passed the test satisfactorily. In Izod "V" notch tests, the impact resistance of exposed pipe was 65% less than that of unexposed pipe. ASTM A 262 boiling nitric acid tests indicated that the piping was sensitized. These changes in mechanical properties are qualitatively consistent with the changes anticipated for Type 316 stainless steel, and

to p. viii



^{Fig. 34}
It is still considered to be a satisfactory material for this service.
Since at least one failure in the system was directly related to excessive external stress, a thorough thermal stress analysis is considered to be essential for any similar new system.

CORROSION EXPERIENCE WITH TYPE 316 STAINLESS STEEL IN SODIUM-POTASSIUM EUTECTIC ALLOY AT 1400°F

I. INTRODUCTION

The Idaho Chemical Processing Plant recovers enriched uranium from spent aluminum-uranium reactor fuels⁽¹⁾ by a solvent extraction process. In the Waste Calcining Facility (WCF) at this plant, Figure 1, highly radioactive waste solutions resulting from this reprocessing are sprayed into a heated bed of fluidized solids where the salts are converted to oxides⁽²⁾. These free-flowing granular solids are produced continuously and are continuously conveyed to permanent storage bins from the calcination reaction vessel through a pneumatic solids transport system. Simultaneously, water vapor and volatile decomposition products are carried over with the fluidizing air to the WCF off-gas cleaning system before being released to the atmosphere. Heat is supplied to the calciner by circulating sodium-potassium (NaK) eutectic alloy through a bayonet heat exchanger in the fluidized solids. Type 316 stainless steel is used as the construction material for this NaK loop.

The NaK loop of the WCF had been in service 25,636 hours as of November 13, 1967. This represents the longest period of operation on record of a Type 316 stainless steel loop with NaK at elevated temperatures. However, some failures have occurred which necessitated extensive analyses of the nature and origin of the failures.

As part of the overall program of surveillance on the stainless steel loop, service tests were conducted on several fittings, on an electromagnetic pump tube, and on a portion of the piping. Metallurgical, electron fractography, chemical, X-ray, and mechanical tests were used during this evaluation of the effects of exposure to NaK at 1400°F.

In the course of these investigations, an insight into the mechanisms of failure of Type 316 stainless steel under these operating conditions was gained. It is clear that failure was not general; that

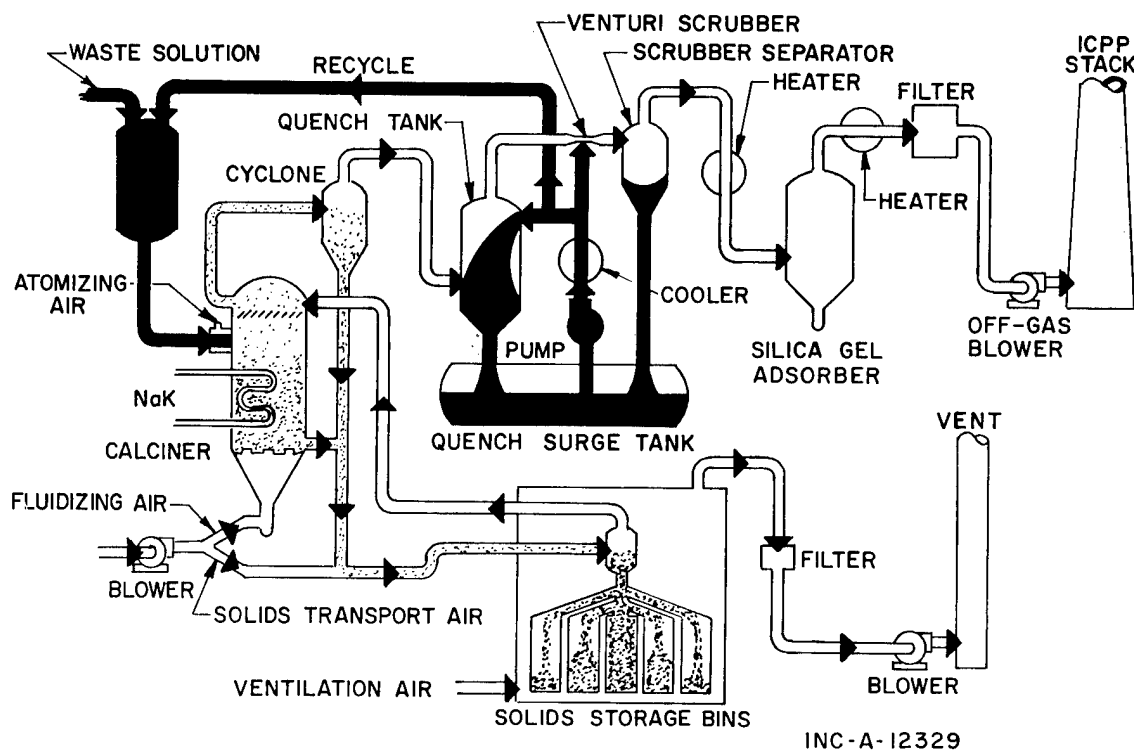


Figure 1 Fluidized bed waste calcining facility.

is, the unstressed, straight runs of pipe did not suffer failure. Rather, failures have occurred in fittings, which, upon close analysis, were shown to have been subjected to considerable external stress, and in cool spots in the loop where mass transfer had produced a high level of carburization. It is imperative that thermal stress analyses be conducted on all complex high temperature loops to avoid excessive external stresses.

Under such a condition, Type 316 stainless steel would again be considered seriously as a material of construction for a similar installation.

To pinpoint the sources of failures, metallurgical, chemical, and engineering analyses associated with each failure of the NaK loop in the WCF are reported in detail in this report, with an interpretation thereof. It should be noted that while pure sodium systems undoubtedly will not behave exactly like the NaK system studied here, and while all austenitic stainless steels will not respond exactly like the Type 316 stainless steel, the same basic mechanisms leading to failure are more or less in action in all such systems. Valuable guidance toward the behavior of other liquid metal systems may be found in the experience reported.

II. GENERAL CONSIDERATIONS ON THE MECHANISMS OF CORROSION IN LIQUID NaK

Prior to discussion of the actual WCF experience, it is pertinent to indicate some generally accepted thoughts concerning the mechanism of structural metal disintegration in liquid NaK and particularly those mechanisms pertaining to Type 316 stainless steel.

1. SENSITIZATION

Sensitization of an alloy is associated with the precipitation of carbides in the grain boundaries wherein the quantity of precipitate is sufficient to form a continuous chromium carbide envelope around each grain. Chemical attack upon steels in this condition could cause granulation or separation of the grains one from another.

The use of extra-low-carbon (ELC) alloys is one method of combating sensitization of austenitic stainless steels. The carbon concentration in ELC alloys is reduced to values where that element presumably does not remove chromium from the grain.

Another method consists of adding to the steel alloying elements such as columbium or tantalum which have greater affinity for carbon than does chromium, leaving the chromium free for passivation. Columbium and tantalum form stable carbides without generally causing other important changes in the alloy. Columbium carbides retain their stability at much higher temperatures than do chromium carbides. These carbides appear and grow to final size during the original solidification and cooling of the ingot, before the chromium has an opportunity to react with the carbon⁽³⁾.

2. SIGMA PHASE FORMATION

In the iron-chromium-nickel austenitic alloy system, a brittle combination of iron and chromium, sigma phase, develops when the austen-

itic alloy is reheated in the temperature range 932-1780°F^(4,5). Loss in ductility and impact resistance, as well as decreased corrosion resistance in certain environments, may follow when sigma phase forms. This is especially the case in alloys containing some ferrite, and particularly in those alloys containing ferritizing elements besides chromium. These ferritizing elements include silicon, molybdenum, titanium, and columbium. Sigma phase may be symbolized as Fe_mCr_n. Theoretically, m and n tend toward equality, but the composition of sigma phase may vary over a wide range.

The occurrence of sigma phase in the austenitic stainless steels depends upon the previous presence of a ferritic phase from which the sigma nucleates⁽³⁾. Its growth is largely confined to the ferrite phase alone. The Type 316 stainless steel that was used in the NaK loop had an analysis of 0.06 percent carbon with 13.40 percent nickel and 16.81 percent chromium. This nickel-to-chromium ratio of 0.8 is somewhat higher than found in typical Type 316 stainless steels⁽³⁾. With the higher nickel-to-chromium ratio in this particular heat, it probably contained more ferrite as milled and was definitely more susceptible to the formation of ferrite in prolonged high temperature service than a Type 316 stainless steel of more typical analysis. Therefore, the formation of sigma phase in this alloy was anticipated. However, sigma phase formation can be induced in any susceptible alloy by severe cold-work followed by an 1800°F heat treatment⁽⁵⁾.

A decrease in impact strength of Type 316 stainless steel is often associated with sigma phase formation. However, the precipitation of carbides can contribute to a decrease in toughness of the Type 316 stainless steel⁽⁶⁾. In the post-service examination of the stainless steel from the NaK loop ϵ -carbide, Fe₂C, was identified by X-ray diffraction. Actually the hexagonal ϵ -carbide is metastable, and when exposed to temperatures above 570°F for a long time, it is converted to the more stable cubic χ -carbide⁽⁷⁾. The ϵ -carbide is thought to be a precursor of χ -carbide (M₂₃C₆) and, though less complete, data indicate that both ϵ - and χ -carbide may be precursors of cementite, Fe₃C⁽⁷⁾. Thus, both chi-phase carbide and cementite presumably would precipitate at the grain boundaries of the piping that was exposed in NaK service and these precipitates contribute to the loss of ductility of the piping.

Based upon existing technology, the use of fully austenitic low-carbon stainless steels is suggested in applications where sigma phase inhibition is highly desirable. Type 316 stainless steel has significantly greater yield and ultimate tensile strength than Type 304L stainless steel after exposure at 1200°F; Type 304L steel has by far the highest impact strength after such exposure^(8,9).

3. MASS TRANSFER

Mass transfer by solution or oxidation processes at various temperatures and velocities of liquid sodium is well known⁽¹⁴⁾. Accordingly, it was expected that some alloying elements of the Type 316 stainless steel loop in the WCF might be removed from the hot region, transferred by the liquid NaK, and finally deposited in the colder regions⁽¹⁰⁾.

In earlier work by others⁽¹¹⁾, a linear increase of mass transfer with velocity up to 15 ft/sec was found by flowing liquid sodium containing 25 ppm oxygen at 1200°F through Type 316 stainless steel specimens of constant bore diameter. At velocities in the range 15 to 40 ft/sec very little increase was observed in the transfer rate. Similar tests with sodium containing 50 ppm oxygen and flowing at 21 ft/sec velocity showed that the mass transfer rate was about equal to rates observed at 25 ppm oxygen flowing at 15 ft/sec velocity. The maximum losses of metal on these Type 316 stainless steel specimens in 25 ppm oxygen were 0.6, 1.1, and 1.8 mils per year (mpy) at sodium velocities of 5, 7 and 12 ft/sec, respectively. In the WCF, the velocity of the NaK in the loop is about 5.6 ft/sec. The oxygen concentration of the NaK in the WCF usually is in the range 30-50 ppm. If the velocity effects of NaK on the Type 316 SS loop are similar to those described for sodium, then the contribution from the velocity of the NaK alone to the overall mass transfer rate in the loop of the WCF could be expected to be near 1 mpy.

Mass transfer has also been detected⁽¹²⁾ in sodium thermal convection loops constructed of Type 316 stainless steel. At fluid velocities of 0.01 to 0.05 ft/sec with sodium containing 50 ppm oxygen, the corrosion rate of the hot leg of a Type 316 stainless steel loop was 0.4 mpy after 2,600 hours at 1600°F. Although this temperature is higher than

that of the NaK in the WCF, the 0.4 mpy rate should be the maximum contribution to mass transfer from semi-quiet areas of the loop, such as the hotter surfaces of the NaK expansion tanks and dead legs.

In a dynamic non-isothermal system, mass transfer rates probably are dependent upon solution-controlled processes. For example, oxides of nickel, iron, and chromium, are formed as well as the oxides of sodium from eutectic NaK⁽¹³⁾. In a recent attempt to explain liquid metal corrosion mechanisms, Horsley⁽¹⁵⁾ showed that the compound $\text{FeO}(\text{Na}_2\text{O})_2$ exists in sodium containing 100 ppm oxygen at temperatures above 1100°F and that this compound decomposes to iron metal and sodium oxide below 1100°F. After the double oxide is nucleated, it could have a long life in the main liquid metal and may dominate the mass transfer process. Assuming that the NaK in the WCF behaves as does liquid sodium, then deposition of metallic iron in the cooler parts of the loop may be expected.

III. NaK LOOP IN THE WASTE CALCINING FACILITY

Liquid NaK (77.2 percent potassium - 22.8 percent sodium) is pumped through three-inch diameter, Type 316 stainless steel, Schedule 40 pipe in a loop which includes an oil-fired radiant heater and a fluidized bed heat exchanger for the 48-inch diameter calciner⁽²⁾ (Figure 2). The loop piping was fabricated from Heat X 22326 at Ellwood Works, National Tube Division, United States Steel Corporation. The specification for this material was ASTM A 312 57-T Grade TP-316, which is detailed in the Appendix. The NaK temperature in the heater reaches a maximum of 1400°F, and decreases to about 1100°F at the outlet of the fluidized bed heat exchanger. The equipment in the loop also includes an electromagnetic pump, expansion tanks, and an oxide removal system. The expansion tanks are vertical cylindrical vessels that permit the NaK to expand when heated; this increase in volume amounts to about 25 percent of the NaK volume at ambient temperature. Thermal insulation used on this loop was designed to be compatible with NaK at 1400°F service temperature, and consists of a 2-inch layer of molded Aerogel (Johns-Mansville Corporation) in contact with the piping and an outer 2-inch layer of 85 percent magnesia.

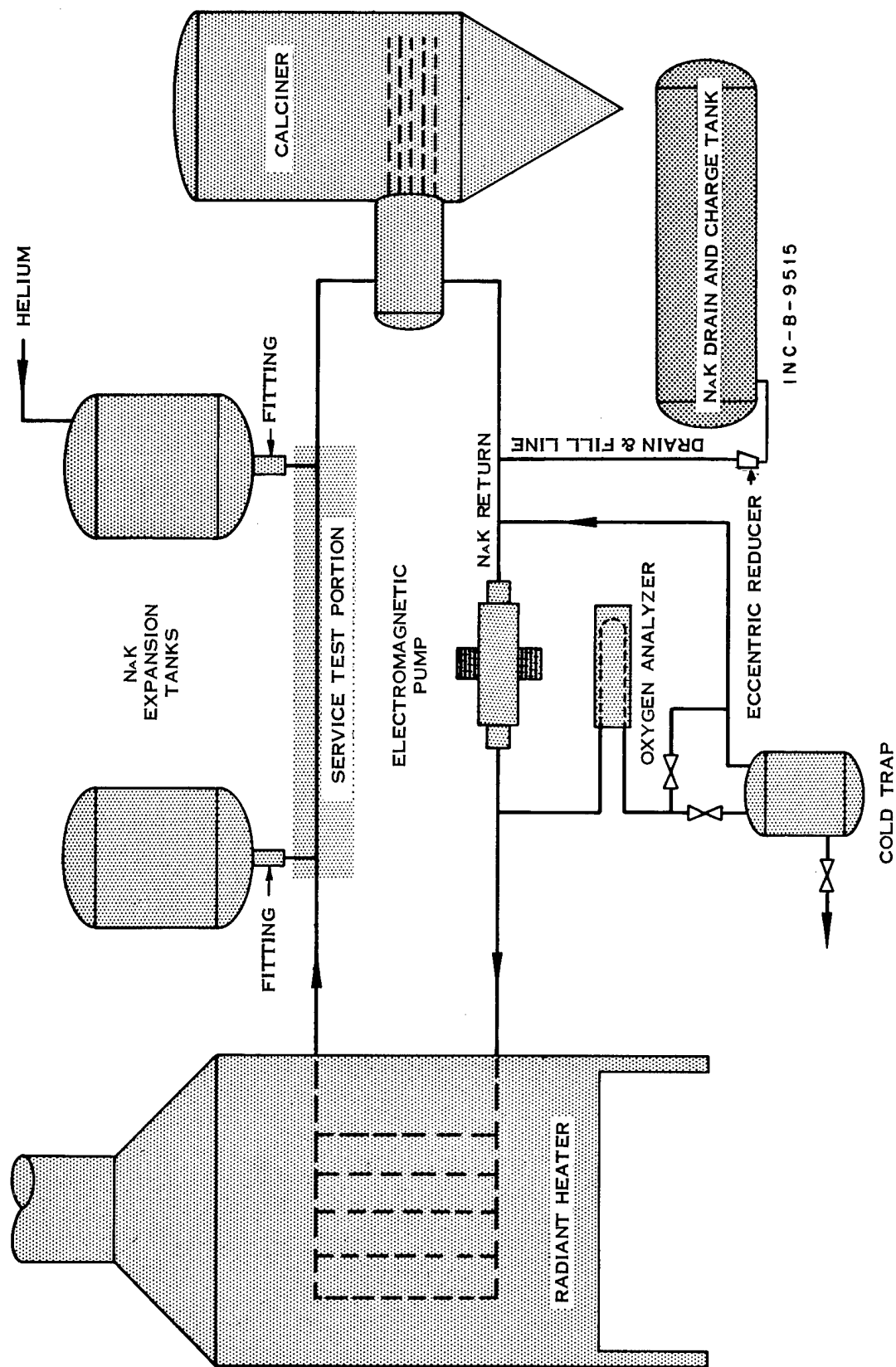


Figure 2 NaK system flow diagram.

IV. EXPERIMENTAL PROCEDURES

Service test examinations were conducted on several fittings, on an electromagnetic pump, and on a portion of piping. After varying time periods, fittings and a pump that had failed in NaK service were examined. A three-inch, Schedule 40 pipe section that was installed upstream from the NaK heater was also examined even though it did not fail.

For results reported in Section V the following experimental techniques were used:

- a. Hardness - Clark diamond pyramid hardness tester on polished cross-sections
- b. Microstructure - photographs of polished cross-sections
- c. Identification of sigma phase, search for other new phases - X-ray diffraction
- d. Carbon and nickel analyses - standard chemical methods
- e. Sensitization - ASTM A 262, Boiling Nitric Acid Test for Corrosion Resisting Steels
- f. Ductility - ASTM A 376, Seamless Austenitic Steel Pipe for High-Temperature Central-Station Service, "Flattening Test"
- g. Tensile strength - a special sheet tensile specimen was cut from exposed pipe wall, as shown in Figure 3, and a tube tensile specimen (Figure 5) was prepared from unexposed tubing from the same heat.
- h. Impact strength - a substandard size specimen (Figure 4) was cut from the pipe wall with the longitudinal axis of the specimen parallel to the longitudinal axis of the pipe. The axis of the ground notch was perpendicular to the surface of the pipe. The standard Izod "V" notch impact test was conducted in air at room temperature.

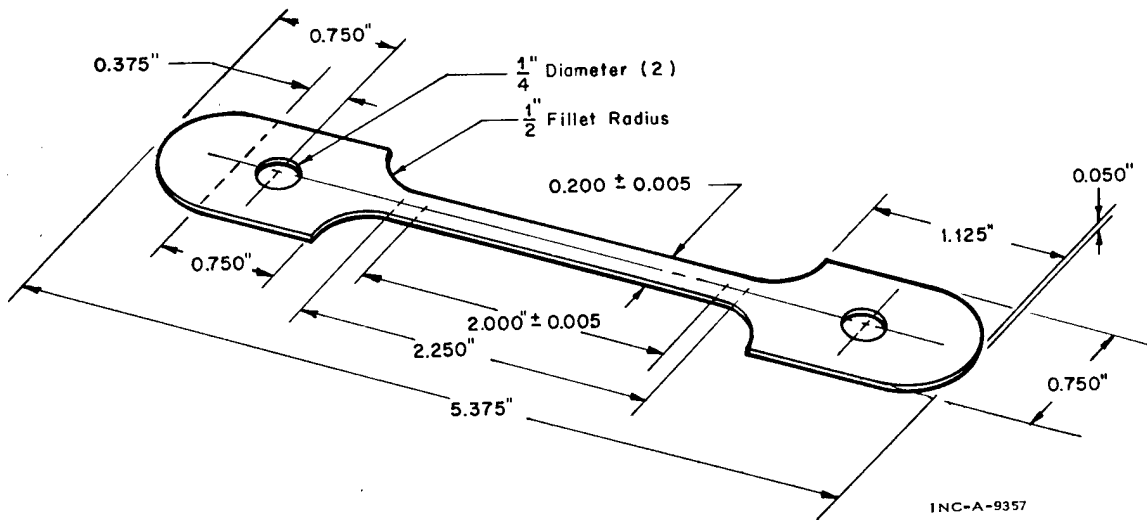


Figure 3 Sheet tensile specimen.

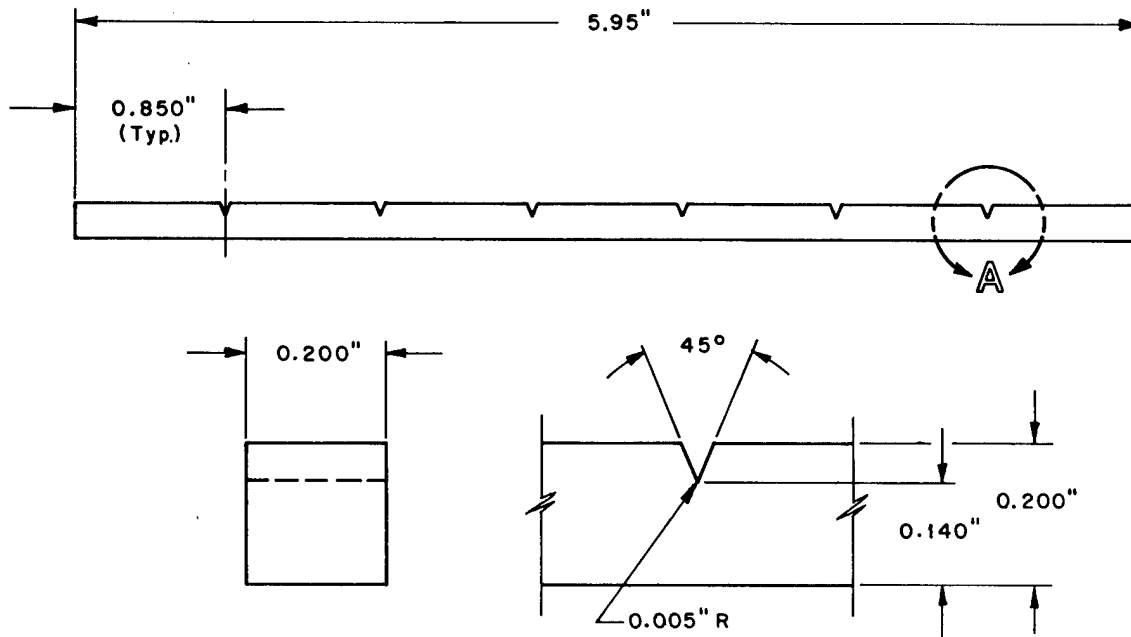


Figure 4 Impact test specimen.

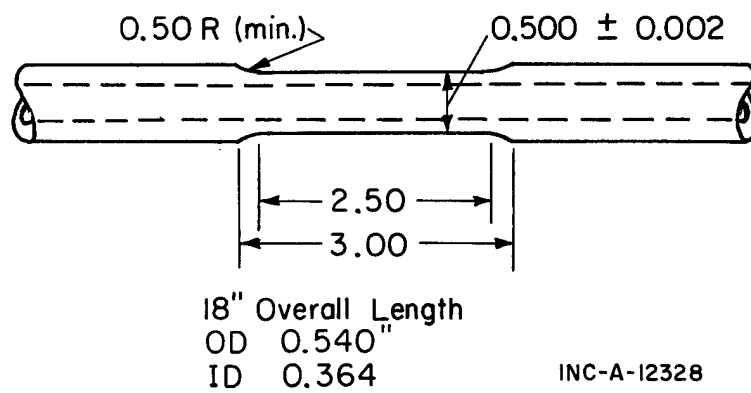


Figure 5 Tube tensile specimen.

V. RESULTS

The Type 316 stainless steel loop used in the WCF was highly satisfactory in NaK service except for a few service-associated effects that were largely eliminated by modifications to the system and could be more nearly completely eliminated by proper design of a new facility. The most significant service-associated effect that was observed in the Type 316 stainless steel was mass transfer; ie, the partial dissolution of certain stainless steel alloy elements in high temperature service areas and deposition of these elements in lower temperature zones. The oxygen that existed in the NaK loop of the WCF is presumed to have been a major contributor to the mass transfer.

Other service-associated effects that were observed in the Type 316 stainless steel of the NaK loop were the formation of sigma phase throughout essentially the whole cross-section of the pipe, and the accompanying evidences of embrittlement. Precipitation of carbides at the grain boundaries was observed, but the associated general corrosion damage was limited to a two-mil thick band of decarburized alloy on the inside surface of the pipe in the high temperature zone and a 0.2-mil thick film of oxide on the outside surface. With present operating temperatures, sigma formation, grain boundary precipitation of carbides, and embrittlement will continue. In fittings where stress was present, serious and extensive cracking occurred. The tensile strength of the exposed metal remained high; but, in the tensile tests, breaking occurred at significantly shorter elongations in the metal exposed to NaK than in unexposed material. Brittle fracture at stressed areas was found to be the most likely mechanism of failure in the fittings.

1. PIPE SECTION

The principal effect that was shown from the post-test evaluation of a piece of pipe from the NaK containment piping system was carbon depletion at the NaK-pipe wall interface. The presence in the piping

of sigma phase formation as evidenced by metallographic examination and accompanying embrittlement are indicative of a fundamental change in the micro structure of the metal due to exposure at elevated temperature.

The pipe section was cut from the hot leg of the loop near the NaK outlet on the oil-fired radiant heater. This section was a 3-inch Schedule 40 pipe that had been in service for 1,118 hours below 1100°F and 15,174 hours above 1100°F, with 37 starts from room temperature.

Chemical analysis of the pipe confirmed that it was Type 316 stainless steel. The average of duplicate carbon and nickel analyses from 5-mil deep turnings were 0.03 and 12.6 percent and 0.09 and 13.2 percent for the inside and outside surfaces of the Type 316 pipe, respectively. General corrosion damage on the specimen after the total of 16,292 hours service was nil.

From X-ray diffraction studies, the presence of sigma was confirmed as a constituent in the exposed piping. The concentration of sigma phase was estimated by use of a planimeter on photomicrographs of the piping sections. Carbide phases that were present in the piping exposed to NaK were not extracted or identified.

The results of ASTM A 262, Boiling Nitric Acid Test for Corrosion-Resisting Steels, on piping that was exposed for 16,292 hours are recorded in Table I. Piping that was tested before the inside and outside surfaces were removed, ie, in the condition existing after NaK exposure, suffered more than 10 mpm corrosion. After 5-mil layers were removed from the inside and outside surfaces, the corrosion rate averaged 1.8 mpm. However, the corrosion rates increased with time on piping that had 5 mils removed from its inside and outside surfaces, so that, at the end of the third period, the rate was 2.7 mpm.

The results of tensile tests at 70°F and 1400°F in air are recorded in Table II. The observed tensile and yield strengths compare favorably with published values on unexposed Type 316 stainless steel. However, the observed average percentage elongations of the exposed pipe were 46 and 63 percent lower than the average of the published values at 70°F and 1400°F, respectively. Izod "V" notch impact test results show that pipe specimens which were in NaK service absorbed 65 percent less kinetic energy in breaking than similarly tested specimens from unexposed pipe.

TABLE I

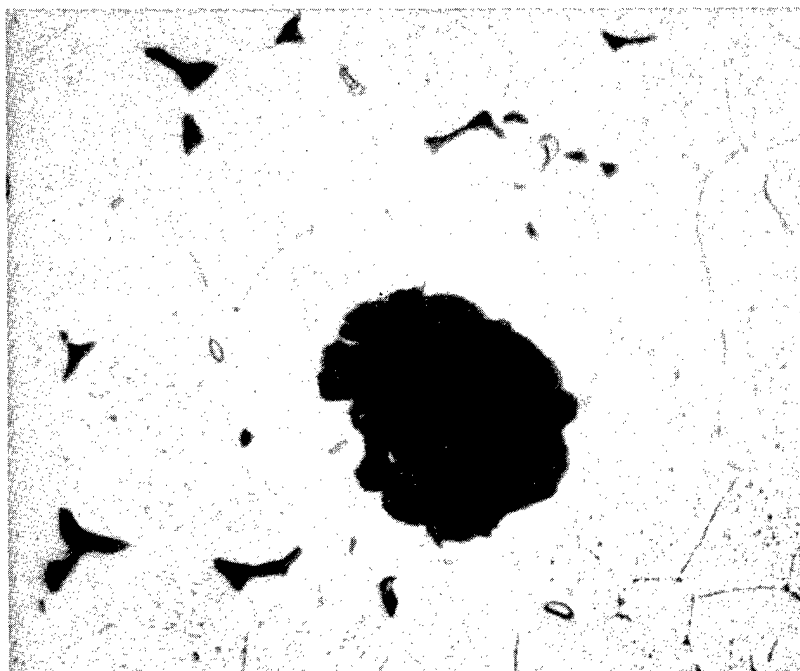
CORROSION OF WROUGHT TYPE 316 STAINLESS STEEL PIPE IN BOILING 65 PERCENT NITRIC ACID AFTER 16,292 HOURS SERVICE IN NaK AT 1400°F

Specimen	Penetration in 48 hr Test Periods				Inter-granular Attack
	1	2	3	Average	
	(mpm)				
Before Removal of Inside & Outside Surfaces	14	10	11	11	Severe
After Removal of Inside & Outside Surfaces	1.1	1.5	2.7	1.8	Mild

Flattening Test, ASTM A 376, Seamless Austenitic Steel Pipe for High-Temperature Central-Station Service, showed that both unexposed and exposed pipe materials were ductile. However, the flattening of a pipe section that was exposed in NaK service at 1400°F for 16,292 hours produced many cracks when the distance between the parallel plates was $1\frac{1}{4}$ inches. Upon continued flattening until the opposite walls of the pipe met, the pipe broke completely into two halves. On the unexposed $2\frac{1}{2}$ -inch long section from 3-inch Schedule 40 Type 316 stainless steel pipe, flattening was continued until opposite walls of the pipe met without breaking the specimen.

The hardness survey showed that the exposed wrought pipe had diamond pyramid hardness (DPH) numbers that ranged from 150 to 180, which correspond to 79 R_b and 87 R_b , respectively. Welds had a hardness of 130 DPH which corresponds to 71 R_b . These values are within the range expected for unexposed Type 316 stainless steel.

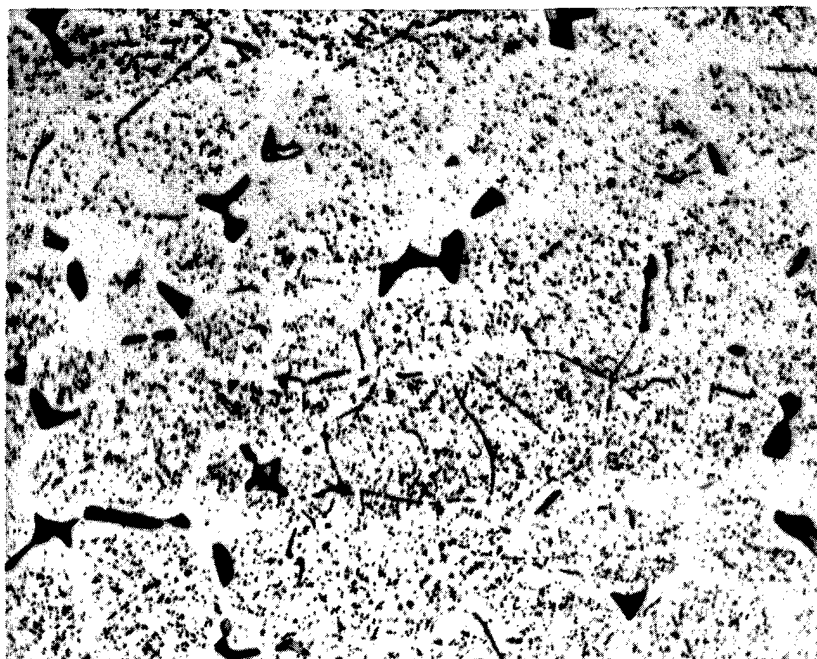
A metallographic examination of the piping indicated carbide precipitation at the grain boundaries and concentrations of up to 11 percent sigma phase as shown in Figures 6 and 7. A band of decarburized material 1 to 2 mils thick, was found on the NaK-side of the pipe wall, as illustrated in Figure 8. A 0.2- to 0.3-mil thick porous oxidation film was observed on the outer surface of the pipe wall, as illustrated in Figure 9. This film was only partially soluble in boiling nitric acid and was magnetic.



10% Oxalic Acid Etch

750X

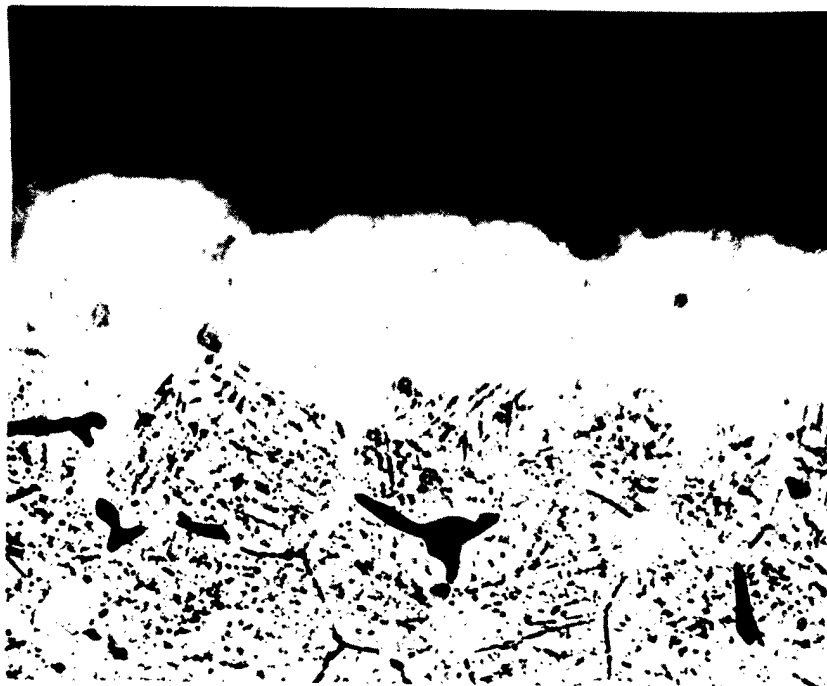
Figure 6 Sigma particle in cross-section of Type 316 ss pipe after 15,000 hours service at about 1400°F. Total Sigma is about 11%.



10% Oxalic Acid Etch

750X

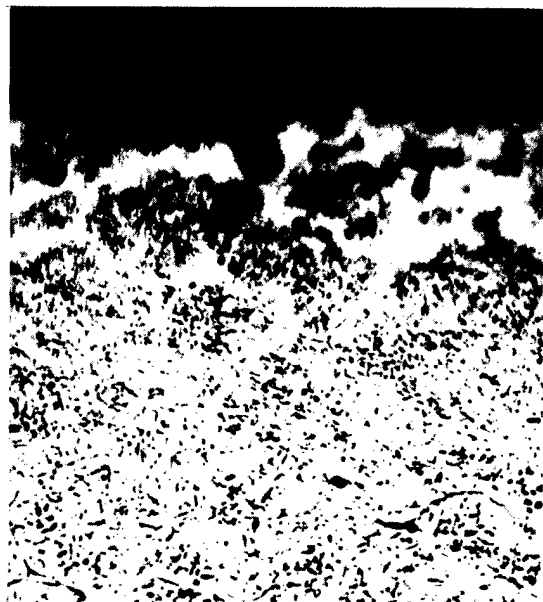
Figure 7 Cross-section of Type 316 ss pipe after 15,000 hours service at about 1400°F. Total Sigma is about 4%.



10% Oxalic Acid Etch

750X

Figure 8 Decarburized zone of inside edge of 3-inch Sch. 40 Type 316 ss pipe after 15,000 hours service at about 1400°F.



10% Oxalic Etch

750X

Figure 9 Air-side of Type 316 ss pipe after 15,000 hours service at about 1400°F.



10% Oxalic Etch

750X

Figure 10 NaK expansion tank weld failure after 3,240 hours at 1100-1400°F service.

TABLE II

MECHANICAL PROPERTIES OF TYPE 316 STAINLESS STEEL

	Tensile Strength (Ksi)(4)	Yield Strength (Ksi)		Elongation in 2 in. (%)	Flattening Test (ASTM A 376)	Subsize Izod Impact (Ft-lb.)
		0.2% Offset	0.1% Offset			
Published Values						
at 70°F	70-110(1)		25-42(2)	40-70(1)	Satisfactory	NA(3)
at 1400°F	30-45(1)			20-60(1)		
Measured Values (after 16,292 Hours in NaK Service)						
at 70°F	96	51	47	30	Failed	3.6
at 1400°F	36	15		14-16		
Tests of Un- exposed Steel (5)						
at 70°F	80	35		63	Satisfactory	10.2
at 1400°F	29	25		54		

(1) ASM Handbook, Vol. 1, 8th Ed., P. 504.

(2) The Elevated Temperature Properties of Stainless Steels, ASTM Data Service Publication DS 5-51, December 1965.

(3) There are no published values since this is not a standard test.

(4) Kilo pounds per square inch.

(5) Using specimens from the same heat of steel from which the WCF piping was fabricated.

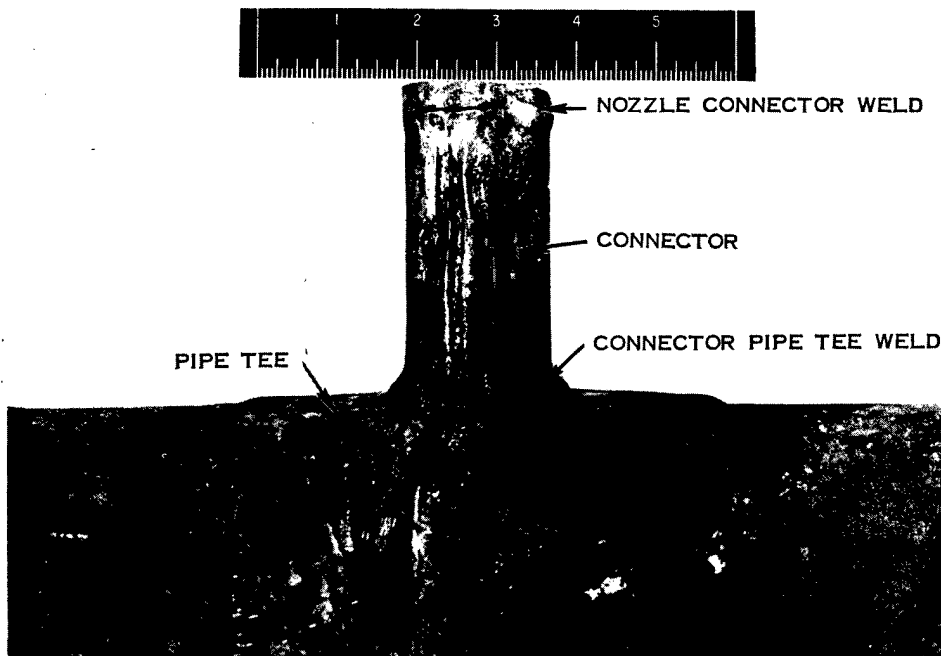
2. FITTINGS

During the post-failure examinations of two pipe tee connectors, cracks were observed in welds; in addition, adjacent piping which was exposed for a total of 17,024 hours was cracked. Cracks were propagated both transgranularly and intergranularly, as shown in Figure 10. Notches which are sites for local stress raisers were found in each of these weld structures.

The investigation of a failure that occurred in the NaK drain pipe indicates that residual and/or applied stresses cracked the eccentric reducer in a manner characteristic of a brittle fracture. The weld joining this forged reducer to the 1½-inch pipe suffered a ductile thermal fatigue fracture.

2.1 Connector Failure After 3,600 Hours Total Service

A service failure occurred at the weld joining a 1½-inch Schedule 40 pipe tee connector and the nozzle of a NaK expansion tank (Figure 11) after 3,240 hours service at 1100-1400°F and 360 hours service below



As received

0.57X

Figure 11 Connector weld failure after 3,240 hours at 1100-1400°F.

1100°F with four starts from room temperature. Type 316 stainless steel was the material of construction of the weld deposit, nozzle, and connector.

Radiographs showed that along the circumference of the root of the weld there was inadequate weld deposit penetration, and incomplete fusion. In addition, mis-alignment and poor beveling of the pipes were observed. A post-failure examination showed hundreds of 10-mil deep marks on the surfaces of the inside pipe shoulders. These marks presumably are tool impressions from a fluted burring reamer that may have been used for removing burrs caused by cutting the piping. In addition, the machining marks on the faces of the two pipes were still evident. An almost continuous combination of both double and triple notches also existed at the pipe-weld-pipe joint.

A microscopic examination of cross sections of the pipe-weld-pipe joint revealed only one crack in the weld and none in the piping. The crack was propagated both through the grains as a transgranular fracture and between the grains as an intergranular fracture, as shown in Figure 10. No plastic deformation of the grains of the weld occurred. No sigma phase or carbide precipitation at the grain boundaries of either the wrought piping or the case weld deposit was found. Electron microscope fractographs of this weld are typified by classic striations or crack arrest lines shown in Figure 12. By comparing this fractograph against published⁽¹⁵⁾ standards, the fatigue failure appeared to be caused by multi-cycle, low stress forces. Evidence of "dimples", typical of ductile fractures, were absent.



2.2 Connector Failure After 17,024 Hours Total Service

During a periodic radiographic inspection of the expansion tanks

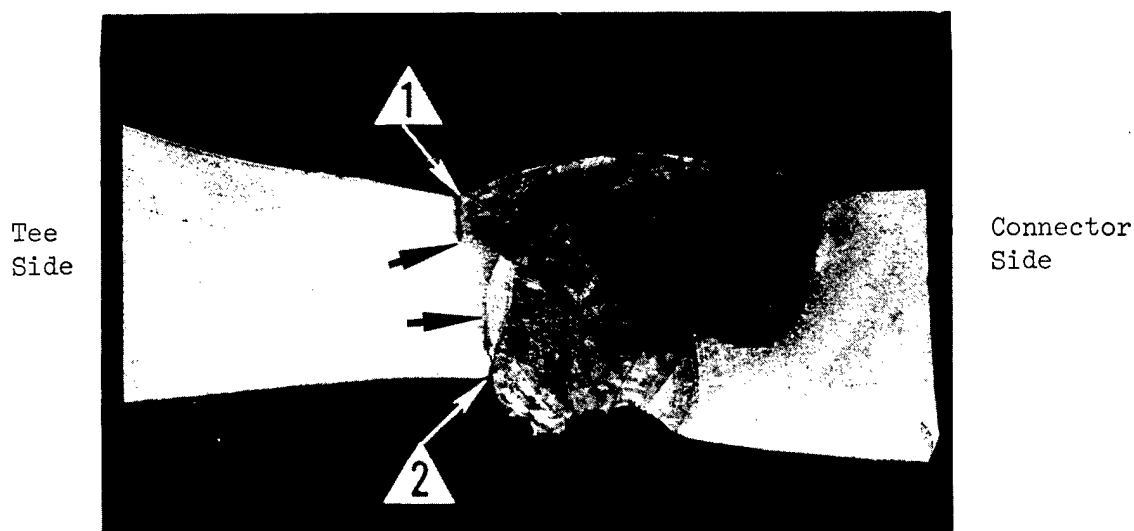
Carbon Replica

14,500X

Figure 12 Surface topography of nozzle-connector weld failure after 3,240 hours at 1100-1400°F showing crack front arrest lines.

in the NaK loop of the WCF, a crack was discovered on the outside and inside of the weld that joined the pipe tee to the connector. This was found after 15,800 hours of service at 1100 to 1400°F and 1,150 hours of service below 1100°F with 39 starts from room temperature.

The crack on the outside of the tee-to-connector weld (tee side) was approximately 0.8-inch long. The crack on the inside of the same weld (also on the tee side) followed the edge of the weld around approximately 75 percent of the circumference. A photograph of these cracks is shown in Figure 13. In this figure, the crack on the outside penetrated 0.053 inches, the inside crack 0.047 inches, with 0.080 inches of sound metal between the crack terminations. The crack on the outside originated at the base of the weld bead at a sharp re-entrant angle. A further inspection showed the presence of a crack on the inner wall of the connector, Figure 14. The crack originating on the outside was lined with an oxide deposit while the inside crack was free of oxide. The three cracks were transgranular, as can be seen in Figures 15 and 16. A second transgranular internal (NaK side) crack, shown also in Figure 14, was found in the wrought pipe that was about ½-inch from the tee-to-connector weld.



10% Oxalic Acid Etch

4.7X

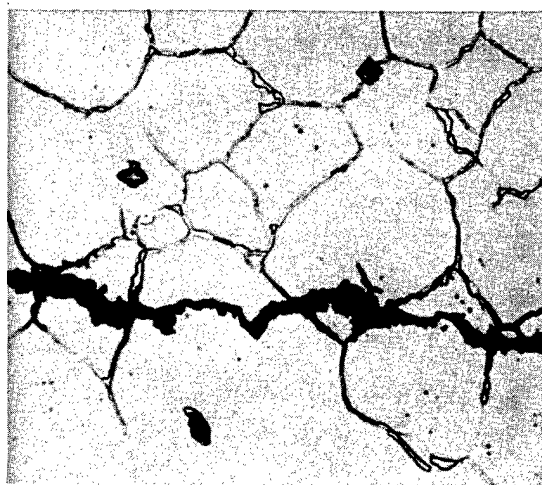
Figure 13 Cross-section through tee connector weld. White arrow 1 shows outside crack. White arrow 2 shows inside crack. Black arrows indicate crack terminations.



10% Oxalic Acid Etch

4.7X

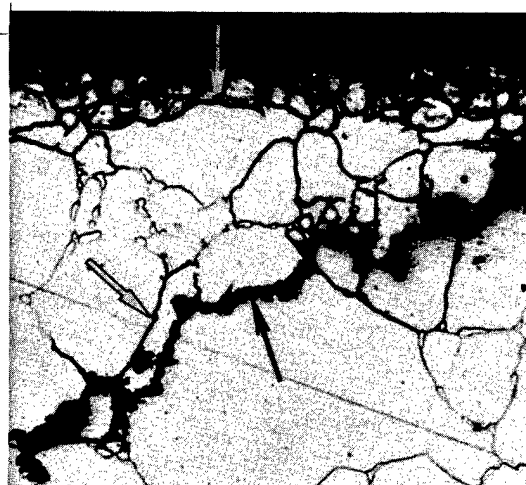
Figure 14 Cross-section through wrought connector. White arrow 1 shows crack on the inside at the base of the weld bead. White arrow 2 shows additional crack found on the inside of the connector. Black arrows indicate crack terminations.



45 Sec. Vilella Etch

500X

Figure 15 Internal crack in wall of pipe tee connector showing transgranular propagation after 15,800 hours service at about 1100-1400°F.



45 Sec. Vilella Etch

500X

Figure 16 Crack on inside of pipe tee connector after 15,800 hours of service at about 1100-1400°F. Fine black lines indicated by white arrows are grain boundaries outlined by etching. Black arrow shows the crack.

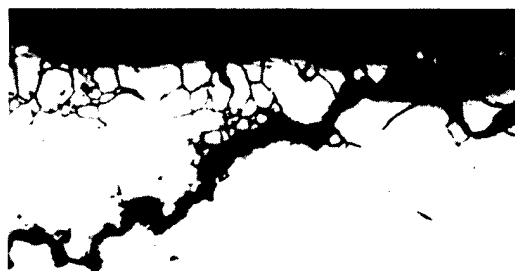
A microhardness survey was made across the wall thickness of both the tee and connector (next to the tee-to-connector weld) with little significant hardness difference being detected. All values were centered around R_p92 . ASM Metals Handbook values for hardness are R_p76 for zero cold work, R_p87 for 10% cold work, and R_p96 for 20% cold work.

Additional metallographic examination of the pipe tee and connector material provided useful information for the evaluation of the effects of the prolonged exposure to high temperatures and NaK. Figures 17 and 18 are identical areas before and after etching with modified Vilella's etch composed of 1 part HF, 2 parts HNO_3 , and 3 parts glycerol. The modified Vilella's etch (~ 15 seconds) attacked a layer of material approximately 0.0008 to 0.001 inch thick on the NaK side of the tee and connector. Etching the same material an additional 30 seconds brought out the structure shown in Figure 19. Three regions are evident--the outer region with the heavy grain boundaries, a second region running from the heavy grain boundary area to the black arrows, and a third one comprising the remainder of the wall thickness. Figure 20 shows the same sample after being repolished and then re-etched with the standard



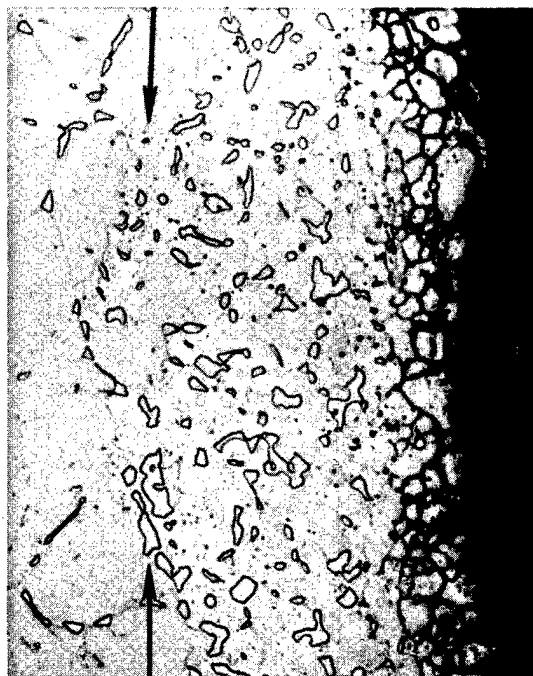
As-polished

Figure 17 Internal crack in wall of connector. (Same area shown in Figure 16.)



500X 15 Sec. Mod. Vilella Etch 500X

Figure 18 Internal crack in wall of connector. (Same area shown in Figure 16.)



45 Sec. Vilella Etch

500X 30 Sec. Vilella Etch

500X

Figure 19 Inside of pipe tee after 15 sec. Mod. Vilella etch and 30 sec. standard Vilella etch. Arrows mark region of structural change.

Figure 20 Inside of pipe tee after 30 sec. standard Vilella etch. Arrows mark region of structural change.

Vilella's etchant for 30 seconds. Standard Vilella's etchant attacks chromium carbides and sigma phase in Type 316 stainless steel at the same rate. Since the outermost layer was not attacked, it seems plausible that a NaK-rich phase was present in the grain boundaries. The second layer contained many larger microconstituents and a few very fine ones. The interior or base metal shown at the left of the black arrows in Figure 19 was representative of the metal all the way to the outer diameter with the exception that the number of large second-phase particles decreased from near the inner diameter (black arrows in Figure 19) to the outer diameter.

By repolishing the samples once more and re-etching with Vilella etchant, sigma phase was tentatively identified as being the large microconstituents shown in Figures 19 and 20. These particles were stained various opalescent colors by Murakami's etchant; thus, further confirming the presence of sigma phase. The fine precipitates evident in Figure 18, are most likely chromium carbides since sigma phase forms

at the expense of chromium carbide. In Figure 20, the layer of material to the right of the black arrows is the decarburized layer generally found in stainless steels exposed to high temperature NaK. This decarburized layer was slightly thinner on the connector than on the tee.

Positive identification of sigma phase was accomplished by X-ray diffraction analysis. A sample of the pipe tee was dissolved in 2:1 hydrochloric-nitric acids. The undissolved residue gave an X-ray diffraction pattern which corresponded to the American Society for Testing Materials (ASTM), X-ray Powder Data File No. 7-356 for sigma phase in molybdenum-titanium 18:8 stainless steel. The residue containing sigma was further dissolved in 48 percent hydrofluoric acid leaving a second residue which was identified by X-ray diffraction as epsilon iron, Fe_2C , that corresponded with ASTM, X-ray File No. 6-0670.

A section of the weld that joined the pipe tee to the connector, containing a representative portion of the inside and outside crack, was opened up by first cutting part way through the weld from the outside. The fracture surface of the inside crack was slightly tarnished and appeared to have been produced much later than the outside crack.

Electron fractography of the two exposed surfaces, as well as the fresh fractures produced by opening the existing cracks, was performed to determine the microscopic topography of the surfaces. Figure 21 shows the topography of the crack found on the outer circumference. The structure can be interpreted as resulting from an overlay of oxide (probably iron oxide) on the surface. Figure 22 shows elongated dimples which are characteristic of a ductile tension fracture. This surface corresponds to the new fracture surfaces produced by opening the existing cracks. The surface features of the crack found on the inner diameter of the weld are shown in Figure 23. The fracture surface was basically quite smooth; although, a number of faceted particles were uniformly distributed. The faceted particles were similar in many respects to the general structure displayed in Figure 21. Chemical analysis of the pipe tee, connector, and weld deposit showed that these were Type 316 stainless steel. The average carbon analysis of turnings from the outside of the connector was 0.06 percent.



Figure 21 Surface topography of outside crack at the pipe tee connector weld.

Carbon replica 14,400X



Figure 22 Surface topography produced by tearing material beyond the crack.

Carbon replica 14,400X

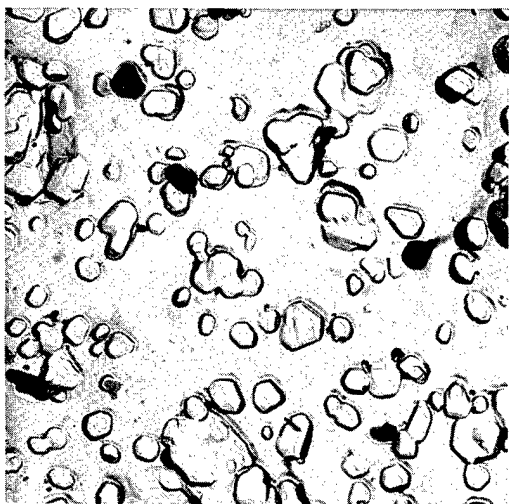


Figure 23 Surface topography of inside crack at the pipe tee connector weld.

Carbon replica 14,400X

2.3 Thermal Stress Analysis

Thermal stress analysis using "General Thermal Pipe Stress and Deflection Program", which was obtained from SHARE General Program Library, showed that stresses would be minimized if the 1½-inch Schedule 40 pipe tee connector for the NaK expansion tank were replaced with a 3-inch Schedule 80 connector. This replacement was made. Freedom of movement of the expansion tanks was needed to prevent thermal stress failure of the tee connector. When cold spring installation was properly used and maintained on the loop, the stresses at the expansion tanks (the points in that part of the system most sensitive to stress) were minimized.

2.4 Failure of Reducer in NaK Drain Piping

An investigation of the failure that occurred in the NaK drain line of the WCF indicated that residual and/or applied stresses cracked an eccentric reducer (Figure 24) in a manner characteristic of a brittle fracture. The weld joining this forged reducer to the 1 1/2-inch pipe suffered a ductile thermal fatigue fracture. Service time on this fitting was 19,080 hours at 1100-1400°F and 1,300 hours below 1100°F. There were 43 starts from room temperature.

Post-failure examination revealed two cracks in the reducer, and another crack in the weld that joined the reducer to the 1½-inch pipe. Both reducer and pipe were Type 316 stainless steel. Figure 24 shows the location of the three cracks. The cracks located at areas 2 and 3 in Figure 24 completely penetrated the forged reducer and weld, respectively, while the turkey-foot crack in area 1 was about 77 mils deep. Both cracks in the reducer were next to welds.

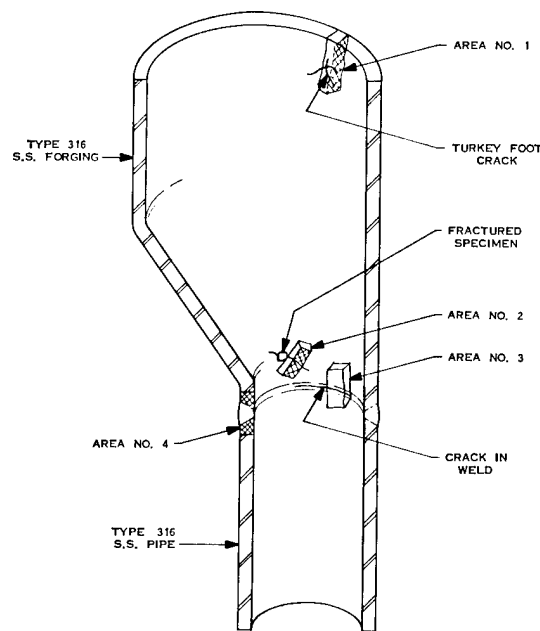
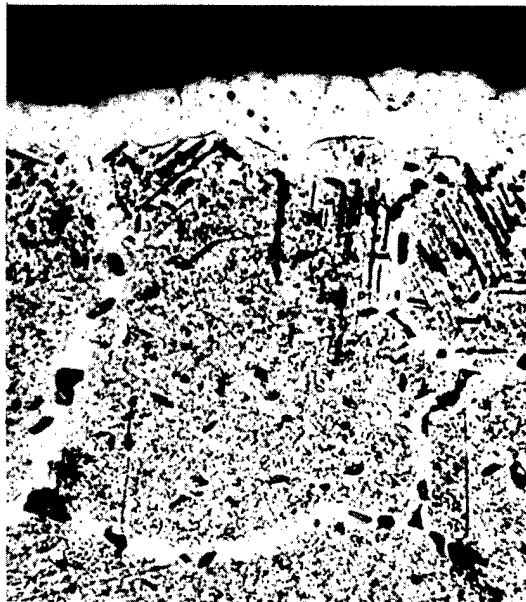


Figure 24 Diagram of 3-inch x 1½-inch eccentric reducer.

A metallurgical study of the reducer and weld at the cracks indicated that a decarburized zone occurred at the NaK stainless steel interface, Figure 25. Some grain dropping was observed in the decarburized zone, Figure 26. Sigma phase was observed at the root of the turkey foot crack, Figure 27, and in a cross-section of the weld in area 4, Figure 28. The massive disintegration of the forging at area 2, together with intergranular fracturing, is shown in Figure 29. A careful inspection of Figures 25 and 27 shows that carbides were precipitated at the grain boundaries of the forged reducer.

Electron microscopic fractographs of the fracture in the weld are typified by elongated dimples, Figure 30. These data suggest that shearing forces were imposed upon the weld, causing a ductile fracture. The fracture in the eccentric formed reducer has a cleavage type profile, Figure 31. This suggests that a brittle fatigue mechanism fractured the reducer.

This failure is another of the series of cracks that have occurred in stressed areas of the NaK piping in the WCF. Forged components, like



10% Oxalic Acid Etch

500X

Figure 25 Decarburized zone of the inside surface of the reducer at Area #1 in Figure 24 after 19,100 hours at about 1100-1400°F.



10% Oxalic Acid Etch

1000X

Figure 26 Grain dropping in the decarburized zone of the reducer at Area #1 in Figure 24 after 19,100 hours at about 1100-1400°F.



Piceral and Hydrochloric
Acid Etch

500X 45 Sec. Vilella Etch

500X

Figure 27 Root of the turkey foot
crack on the inside surface of the
reducer at Area #1 in Figure 24
showing sigma phase formation after
19,100 hours at about 1100-1400°F.



Figure 28 Weld at Area #4 in Figure
24 showing sigma phase formation
after 19,100 hours at about 1100-
1400°F.



45 Sec. Vilella Etch

25X Carbon Replica

7700X

Figure 29 Cross-section of forging
at Area #2 in Figure 24 showing
intergranular fracturing after
19,100 hours at about 1100-1400°F.

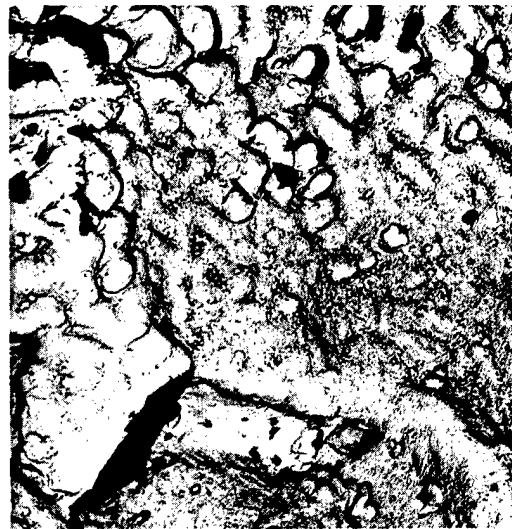


Figure 30 Surface topography of the
weld failure at the reducer to 1-
inch pipe after 19,100 hours service
at 1100-1400°F showing elongated
dimples of ductile fatigue.

the tee connectors and this reducer, appear to be particularly susceptible to attack, either because of location and stress concentration or because of metallurgy.

3. ELECTROMAGNETIC PUMP

A perforation developed on the suction side of the electromagnetic NaK pump tube located upstream from the cold trap. This failure occurred after 20,136 hours of service at 1022 to 1100°F and 1,295 hours below 1022°F, with 44 starts from room temperature.

After dismantling the field coil, current transformers, and primary coils, a pin-hole was observed on top of the suction side of the pump tube just under the mica which insulates the field coil from the tube as shown in Figures 32 and 33. Using a 1/4-inch fly-cutter, the tube was machined to expose the NaK side of the pin-hole, Figures 34A, 34B, and 34C.

A pit was located on the tube wall just opposite the pin-hole, as shown in Figures 34A and 34C. Cross-sections of the pin-hole and pit are shown in Figures 35 and 36, respectively. A section of the pump tube at two different magnifications is shown in Figures 37 and 38. The darkened band on the NaK side of the tube indicates carburization to a depth of 6 to 12 mils.

From X-ray diffraction studies, the carburized band was characterized as almost 100 percent alpha iron; silicon carbide was a minor crystalline component of the band. Chemical analysis confirmed that the pump tube material was Type 316 stainless steel.

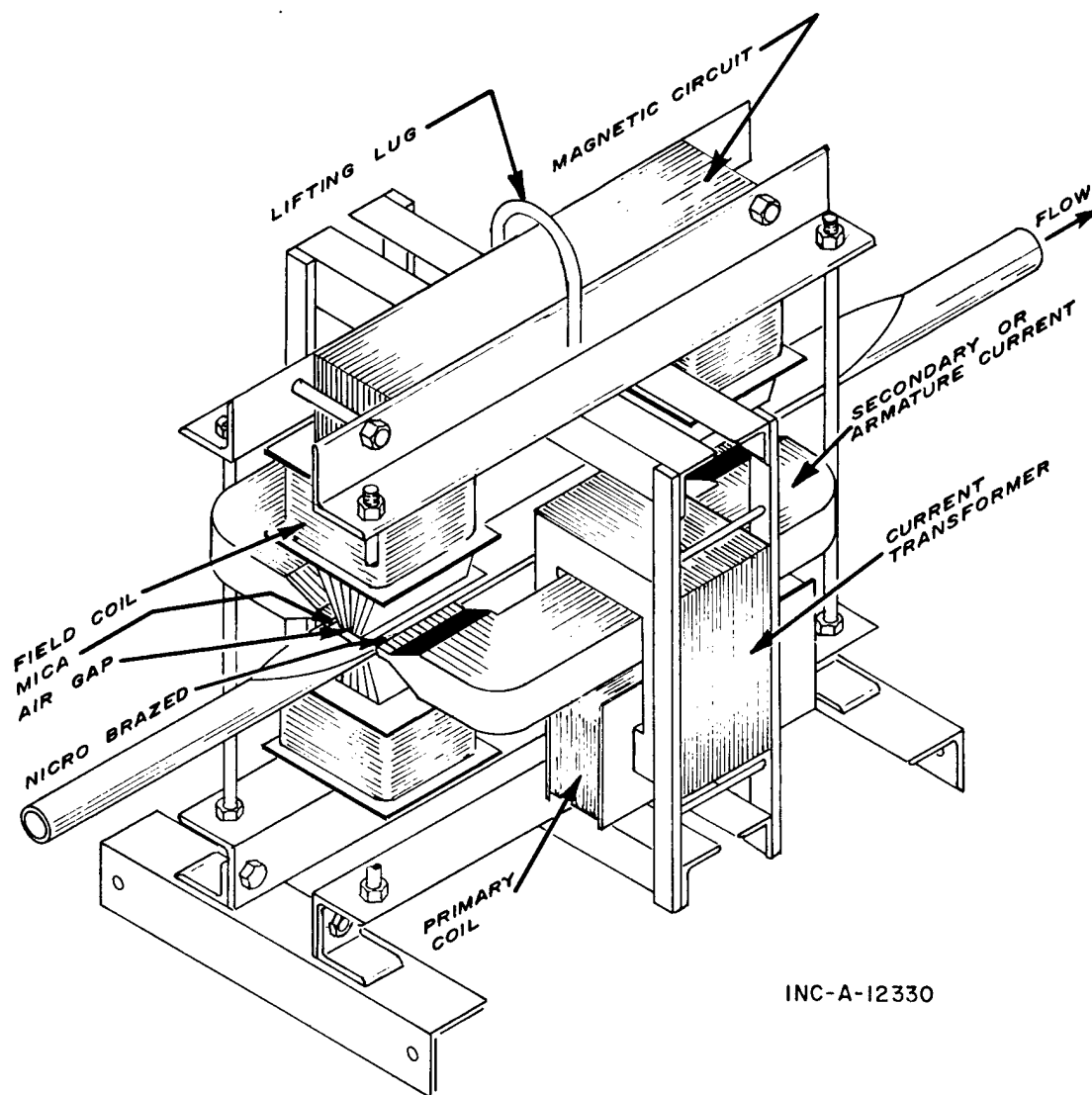
The carburized band was examined for chromium, nickel, and molybdenum with a microprobe. Results



Carbon Replica

7700X

Figure 31 Surface topography of the crack of the forged reducer at Area #2, after 19,100 hours service at about 1100-1400°F showing both elongated or tear dimples of ductile fatigue and intergranular brittle fatigue.



INC-A-12330

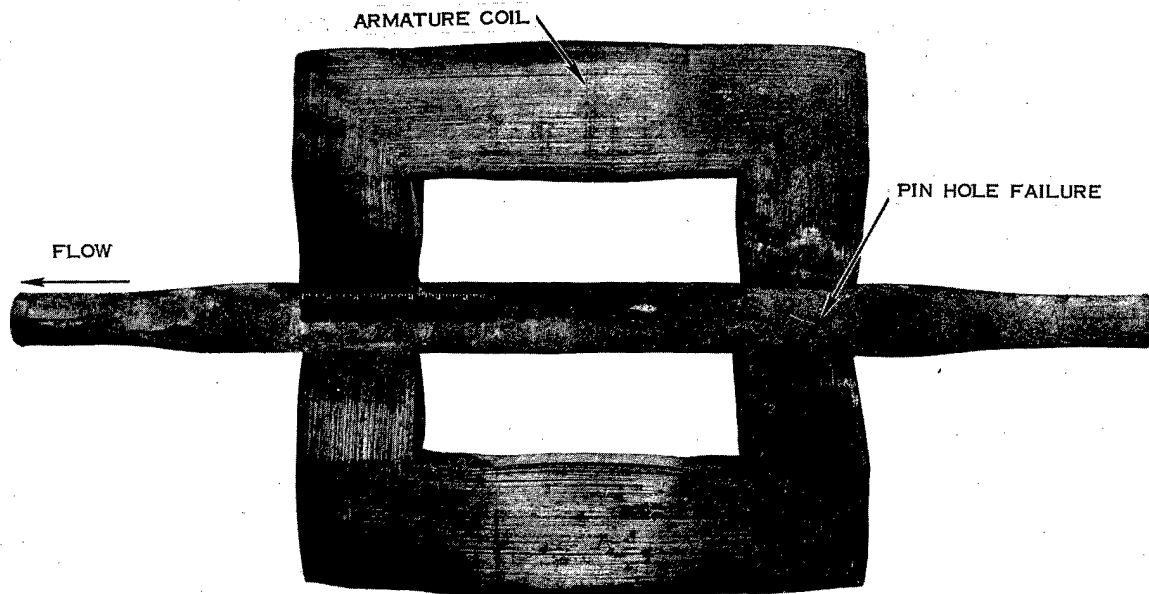
Figure 32 NaK electromagnetic pump.

showed that these elements were lower in concentration at the carburized band than in the underlying Type 316 stainless steel. Chromium concentration in the band was 20 to 33 percent less than that in the base metal of the Type 316 stainless steel tube. Nickel concentration was constant throughout the various carburized regions but amounted to only 80 percent of that in the base tube; the molybdenum concentration was 50 percent of that found in the tube.

The average of duplicate chemical analyses for carbon, chromium, nickel, and molybdenum of $2\frac{1}{2}$ -mil deep chips from the inside flattened surfaces of the pump tube were 1.5, 18.8, 8.7, and 1.6 percent, respectively. These chips were highly magnetic. The next successive

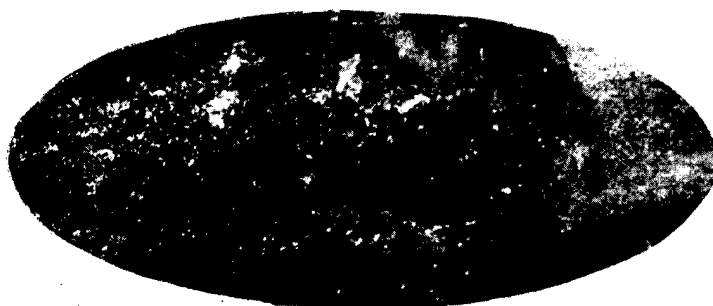
2-mil deep machined chips contained 0.14 percent carbon and the final 2-mil deep chips contained 0.10 percent carbon.

There is no complete explanation for this failure; although, there is considerable evidence of carburization of the pump tube, and this is an area where cavitation could occur.

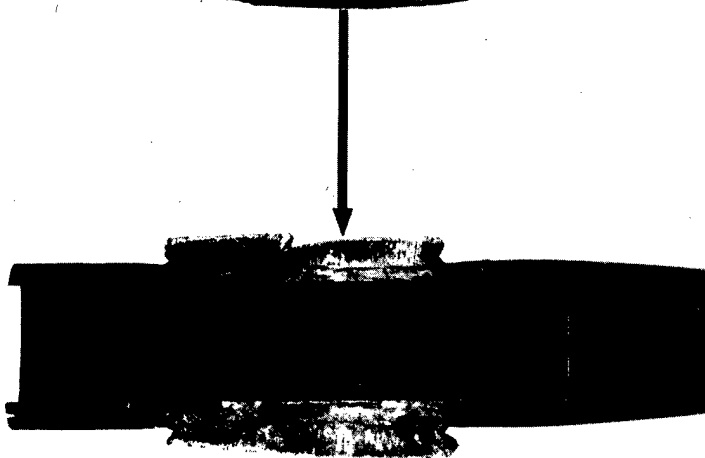


As received.

Figure 33 Dismantled NaK electromagnetic pump tube and armature coil.



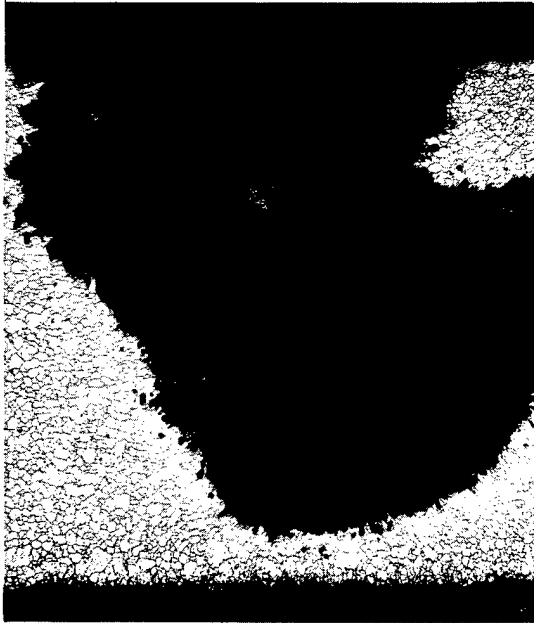
Unetched 4X
Figure 34B Inside surface
of pin hole failure of the
EM pump tube.



Unetched .25X
Figure 34A Inside surface
of NaK EM pump tube after
20,100 hours at 1022-1400°F.



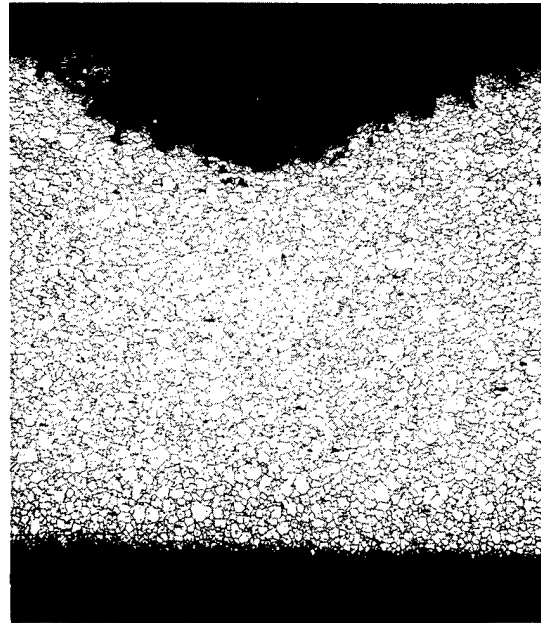
Unetched 4X
Figure 34C Inside surface
opposite the pin hole of
the EM pump tube.



30 Sec. Vilella Etch

25X

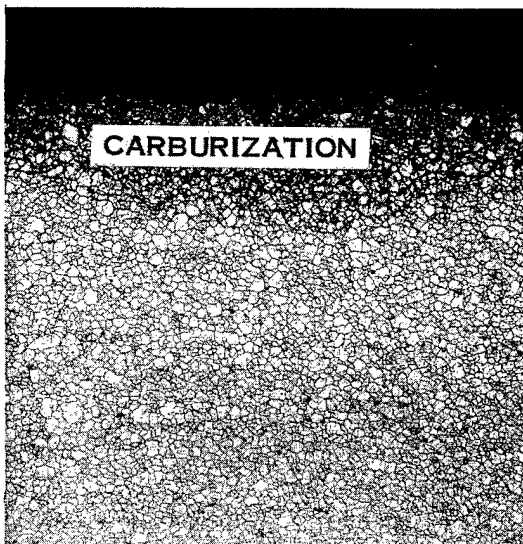
Figure 35 Cross-section of pin-hole in NaK pump tube after 20,100 hours at about 1022-1100°F.



30 Sec. Vilella Etch

25X

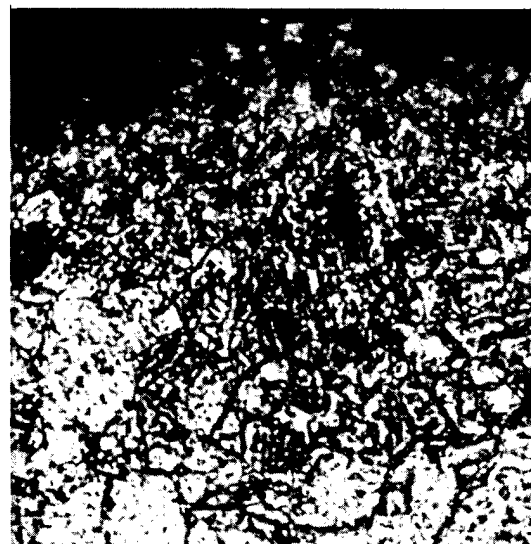
Figure 36 Cross-section of pit in NaK pump tube after 20,100 hours at about 1022-1400°F.



30 Sec. Vilella Etch

25X

Figure 37 Cross-section of EM pump tube showing a carburization band on the NaK side of pump tube after 20,100 hours at about 1022-1100°F.



30 Sec. Vilella Etch

700X

Figure 38 Cross-section of EM pump tube showing carburization on NaK side of pump tube after 20,100 hours at about 1022-1100°F.

VI. CONCLUSIONS

The results of this work suggest that Type 316 stainless steel is a suitable material of construction for ^{start} non-isothermal loops containing NaK at 1100-1400°F. However, stress analysis of the piping should be made during design of such loops since there appears to be a relationship between failure and applied stress on the components of the loop. The presence of sigma phase, which increases in concentration with exposure time at the elevated temperatures, does not appear to greatly affect the servicability of the steel as long as the sigma particles are small and dispersed, but the accompanying embrittlement may lead to failure in areas of high external stress. Carburization, clearly associated with mass transfer in the non-isothermal loop, was in part the cause of failure of the pump tube in the WCF system. Other metallurgical changes or corrosion effects were either undetectable or did not influence the performance of the steel. |

end

VII. REFERENCES

1. K. L. Rohde, Performance of the TBP Process for Aluminum Fuels - Idaho Chemical Processing Plant, USAEC Report, IDO-14427 (January 1958).
2. J. A. McBride, J. A. Buckham, J. R. Hoffman, ICPP Waste Calcining Facility Safety Analysis Report, USAEC Report, IDO-14620 (December 1963).
3. C. A. Zapfee, Stainless Steel, ASM, Chapters II, III and IV (1949).
4. H. W. Kirkby, and J. I. Morlay, "The Formation of Sigma Phase in Duplex Chromium-Nickel-Molybdenum Corrosion Resisting Steels," Journal of the Iron and Steel Institute, Vol. 158 (March 1948), pp. 289-294.
5. L. Smith and K. W. J. Brown, "The Occurrence of Some Effects of Sigma Phase in a Molybdenum-Bearing Chromium-Nickel Austenitic Steel," Journal of the Iron and Steel Institute, Vol. 158 (March 1948), pp. 295-305.
6. L. H. Cope, United Kingdom Atomic Energy Authority, The Reactor Group, The Physical and Mechanical Properties of AISI Types 316 and 316L Stainless Steel, IRG-283, (December 19, 1962).
7. C. E. Spaeder and K. G. Bricker, "Modified Type 316 Stainless Steel with Low Tendency to Form Sigma," Advance in the Technology of Stainless Steels and Related Alloys, ASTM, Special Technical Publication No. 369 (March 1963), p. 143.
8. M. Manes, et al, "Hexagonal Iron Carbides as an Intermediate in the Carbiding of Iron Fisher-Tropsch Catalysts," The Journal of the American Chemical Society, Vol. 74 (December 20, 1952) pp. 6207-6209.
9. M. T. Simnad, The Stability and Properties of Alloy Steels at Elevated Temperatures-A Literature Survey, USAEC Report, GAMD-1796 (November 21, 1960) p. 72.
10. T. L. Hoffman, Performance of Types 304, 316 and 348 Stainless Steel in NaK at High Temperatures, USAEC Report, IN-1089 (May 1967).
11. C. A. Zimmerman, Corrosion of Type 316 Stainless Steel in NaK Service--A Literature Survey, USAEC Report, IDO-14651 (February 1965).
12. A. W. Thorley and C. Tyzaer, United Kingdom Atomic Energy Authority, The Reactor Group, Culcheth, Warrington, Lancashire; The Corrosion Behavior of Steels and Nickel Alloys in High Temperature Sodium, NP 16413, (1966).
13. W. R. Holman, Mass Transfer By High Temperature Liquid Sodium, USAEC Report, AECU-4072 (October 15, 1958).

14. D. D. Williams, J. A. Grand, and R. R. Miller, "Determination of the Solubility of Oxygen Bearing Impurities in Sodium, Potassium, and Their Alloys," Journal of Physical Chemistry, Vol. 63 (January 1959) pp. 68-71.
15. G. W. Horsley, "Corrosion of Iron by Oxygen-Contaminated Sodium," Journal of the Iron and Steel Institute, Vol. 182 (January 1956) pp. 43-48.
16. A. Phillips, et al, Electron Fractograph Handbook, Air Force Materials Laboratory, Wright-Patterson Air Force Base, AD612912 (January 31, 1965).

APPENDIX

ANALYSIS & TENSILE STRENGTH OF STEEL USED IN THE WASTE CALCINING FACILITY

NATIONAL TUBE

ELLWOOD WORKS

DIVISION
UNITED STATES STEEL CORPORATION

CUSTOMER'S ORDER 60100 PMS 2 SPECIFICATION ASTM A-312-57-T Grade TP 316

N. T. DIV. ORDER US 00565 DATE January 28, 1959

SIZE 3.500" OD x .216" wall

Invoice No. Pieces

H 9988 18

MATERIAL NATIONAL SHELBY SEAMLESS TUBING

LOT NO.	CHEMICAL ANALYSIS							PHYSICAL PROPERTIES			CRUSH TEST	REMARKS	
	CAR.	MANG.	PHOS.	SUL.	SIL.	NI.	CR.	MO	Ti.	ULTIMATE STRENGTH			YIELD POINT
Hydro. Test 1900#	.06	1.55	.030	.019	.38	13.40	16.81	2.20		81750	46120	54.0	Heat No. X22326
The flattening tests were satisfactory.													

THE FLUOR CORP.
NRTS IDAHO

FEB - 4 1959

FILE
INFO
ACTION
REPLY

CONTRACT

5799

GEN. SUPT.

SUPT.

SUFT. MGR.

OFF. PURCH.

CH. MTLMAN

JOB ENGR.

PERSONNEL

THE FLUOR CORP.
NRTS IDAHO
FEB - 4 1959

FILE INFO	
ACTION	
REPLY	
CONTRACT	
5799	
GEN. SUPT.	
SUPT.	
OFF. MGR.	
PURCH.	
CH. MTLMAN	
JOB ENG.	
PERSONNEL	

THE ABOVE ANALYSIS & TENSILE PROPERTIES ARE CORRECT & TO THE BEST OF MY KNOWLEDGE & BELIEF.

SWORN & SUBSCRIBED BEFORE

ME THIS 28th day of January, 1959

Margaret M. Duffey
MARGARET M. DUFFEY, NOTARY PUBLIC,
ELLWOOD CITY, LAWRENCE COUNTY, PA.
MY COMMISSION EXPIRES MAY 22, 1961

SIGNED:

METALLURGIST

W. A. Duff